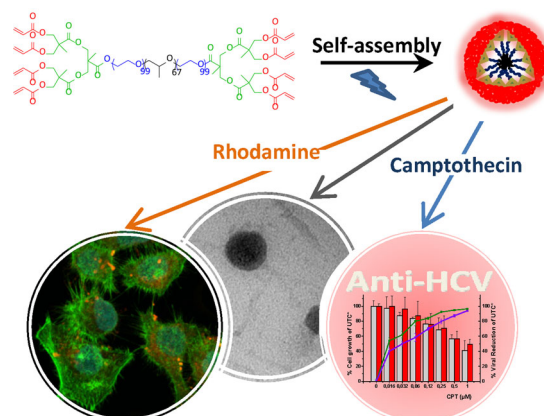


Shell Cross-Linked Polymeric Micelles as Camptothecin Nanocarriers for Anti-HCV Therapy^a

Isabel Jiménez-Pardo, Rebeca González-Pastor, Alexandre Lancelot, Rafael Claveria-Gimeno, Adrián Velázquez-Campoy, Olga Abian, M. Blanca Ros,* Teresa Sierra*

A suitable carrier for camptothecin to act as therapy against the hepatitis C virus is presented. The carrier relies on an amphiphilic hybrid dendritic–linear–dendritic block copolymer, derived from pluronic F127 and bis-MPA dendrons, that forms micelles in aqueous solution. The dendrons admit the incorporation of multiple photoreactive groups that allow the clean and effective preparation of covalently cross-linked polymeric micelles (CLPM), susceptible of loading hydrophilic and lipophilic molecules. Cell-uptake experiments using a newly designed fluorophore, derived from rhodamine B, demonstrate that the carrier favors the accumulation of its cargo within the cell. Furthermore, loaded with camptothecin, it is efficient in fighting against the hepatitis C virus while shows lower cytotoxicity than the free drug.



1. Introduction

Among the various nanocarriers described and assayed as for drug delivery systems,^[1] cross-linked polymeric

micelles (CLPM), formed by amphiphilic block copolymers, have been successful for biomedical applications.^[2] First, they can fulfill those general requirements for drug delivery systems: water solubility, low toxicity, to

Dr. I. Jiménez-Pardo, Prof. M. B. Ros, Dr. T. Sierra
Departamento de Química Orgánica, Instituto de Ciencia de
Materiales de Aragón (ICMA) - Universidad de Zaragoza-CSIC,
50009, Zaragoza, Spain
E-mail: bros@unizar.es
E-mail: tsierra@unizar.es
R. González-Pastor, R. Claveria-Gimeno, Dr. A. Velázquez-Campoy,
Dr. O. Abian
Instituto de Investigaciones Sanitarias de Aragón (IIS-Aragón),
50009, Zaragoza, Spain
R. González-Pastor, R. Claveria-Gimeno, Dr. O. Abian
Instituto de Ciencias de la Salud (IACS), 50009, Zaragoza, Spain

A. Lancelot
Departamento de Química Orgánica, Instituto de Nanociencia de
Aragón, Universidad de Zaragoza, 50018, Zaragoza, Spain
R. Claveria-Gimeno, Dr. O. Abian
Centro de Investigación Biomédica en Red en el Área Temática de
Enfermedades Hepáticas y Digestivas (CIBERhd), Barcelona,
Spain
R. Claveria-Gimeno, Dr. A. Velázquez-Campoy, Dr. O. Abian
Institute of Biocomputation and Physics of Complex Systems
(BIFI), Joint Unit IQFR-CSIC-BIFI, Universidad de Zaragoza, 50018,
Zaragoza, Spain
Dr. A. Velázquez-Campoy
Fundación ARAID, Government of Aragón, 50018, Zaragoza, Spain

^aSupporting Information is available from the Wiley Online Library or from the author.

increase the stability of the drug inside the living organisms, to facilitate cellular uptake compared to free drug, and to produce its controlled release at a specific location. Second, the amphiphilic nature of the constituent polymer results in a hydrophobic core and a hydrophilic shell that allow encapsulation of both types of drug. Third, these nanoparticles offer further stability under high dilution conditions, below the critical micellar concentration, compared to other polymeric micelles. Indeed, cross-linking avoids its disintegration in the bloodstream and the release of the drug before reaching the target cell. Particularly, fixation of the micelle structure by light-induced covalent cross-linking, mostly employing acrylate reactive groups,^[3] represents a clean and effective procedure to prepare stable polymer micelles that can hold either water-soluble and non-water soluble molecules and transport them through the bloodstream.

The features of nanocarriers, in general, and polymeric micelles, in particular, have been successfully leveraged for anticancer therapies,^[4] but are also attractive, and not extensively applied, for the development of systems to treat viral diseases.^[5] In this respect, camptothecin (CPT), a poorly water-soluble drug extracted in 1966 from the plant *Camptotheca acuminata*, which exhibits remarkable anticancer activity against different types of cancer,^[6] has been recently described as a potent antiviral agent for hepatitis C virus (HCV).^[7] Indeed, a novel high throughput screening (HTS) strategy for identifying potential antivirals led to the identification of this new potential pharmacological use of CPT.^[8] However, CPT has some drawbacks that limit its applications, i.e., very low water solubility^[9] and chemical instability due to hydrolysis of its lactone ring under physiological conditions. To overcome this issue, different strategies have been adopted by researchers and several carriers for CPT have been described.^[10] Nevertheless, none of them have been explored for their potential for antiviral therapies.

We herein present a new shell CLPM that shows high loading capacity for camptothecin while maintaining its antiviral activity and decreasing toxic effects.

Based on our previous results about effective nanocarriers for antiviral drugs,^[11] we have selected a hybrid dendritic-linear-dendritic block copolymer (HDLDBC) structure^[12] for the design of a suitable amphiphilic macromer to form polymeric micelles with a hydrophobic core and a hydrophilic cross-linkable shell (Figure 1). As for

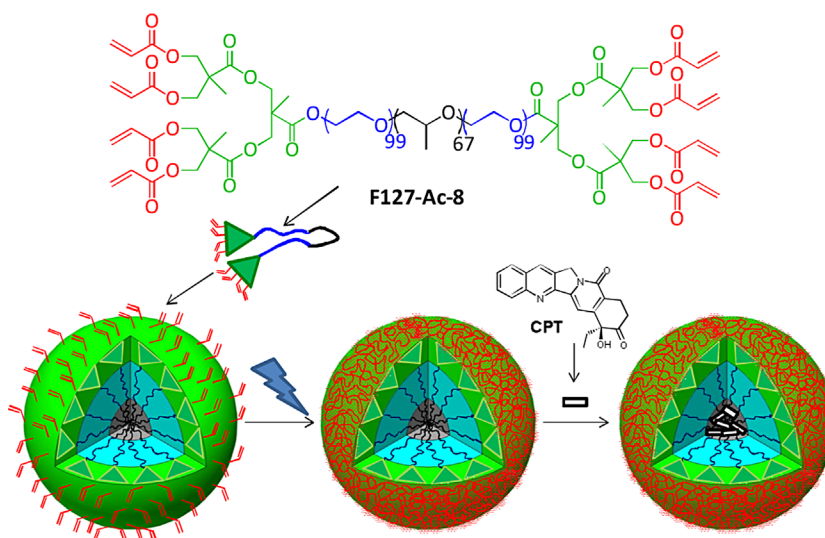


Figure 1. Chemical structure of the macromer F127-Ac-8. Schematic representation of micelle formation, shell-photocross-linking, and CPT loading.

the lineal moiety, Pluronic F127 offers the ability to self-arrange in aqueous solutions forming micelles, which have proven to be excellent candidates for the physical encapsulation of hydrophobic drugs,^[13] with enhanced drug transport across cellular barriers.^[14] This lineal block copolymer is functionalized at both ends with dendritic blocks. The characteristic multivalency of dendritic blocks affords the possibility of multifunctionalization with photoreactive groups in the periphery to permit micelle shell-photocross-linking. Dendritic blocks are based on 2,2-bis(hydroxymethyl) propionic acid (*bis*-MPA) that provides a biocompatible and biodegradable scaffold.^[15] In vitro cell-experiments have demonstrated that these nanoparticles permit the accumulation of their cargo within the cell using rhodamine B as a fluorescent probe. To further confirm cell internalization of the polymeric micelles, a new rhodamine B derivative with poor water solubility has been prepared to prevent fast release during the cell-internalization experiment. Finally, the potential of these nanoparticles as drug carriers for anti-HCV therapy has been studied with the poorly water-soluble drug CPT demonstrating that non-toxic CPT-loaded systems display similar anti-HCV activity than free, and more toxic, CPT.

2. Results and Discussion

2.1. Synthesis and Characterization of the Amphiphilic HDLDBC Macromer

The macromer F127-Ac-8 was synthesized by divergent growing of second-generation *bis*-MPA dendrons at both

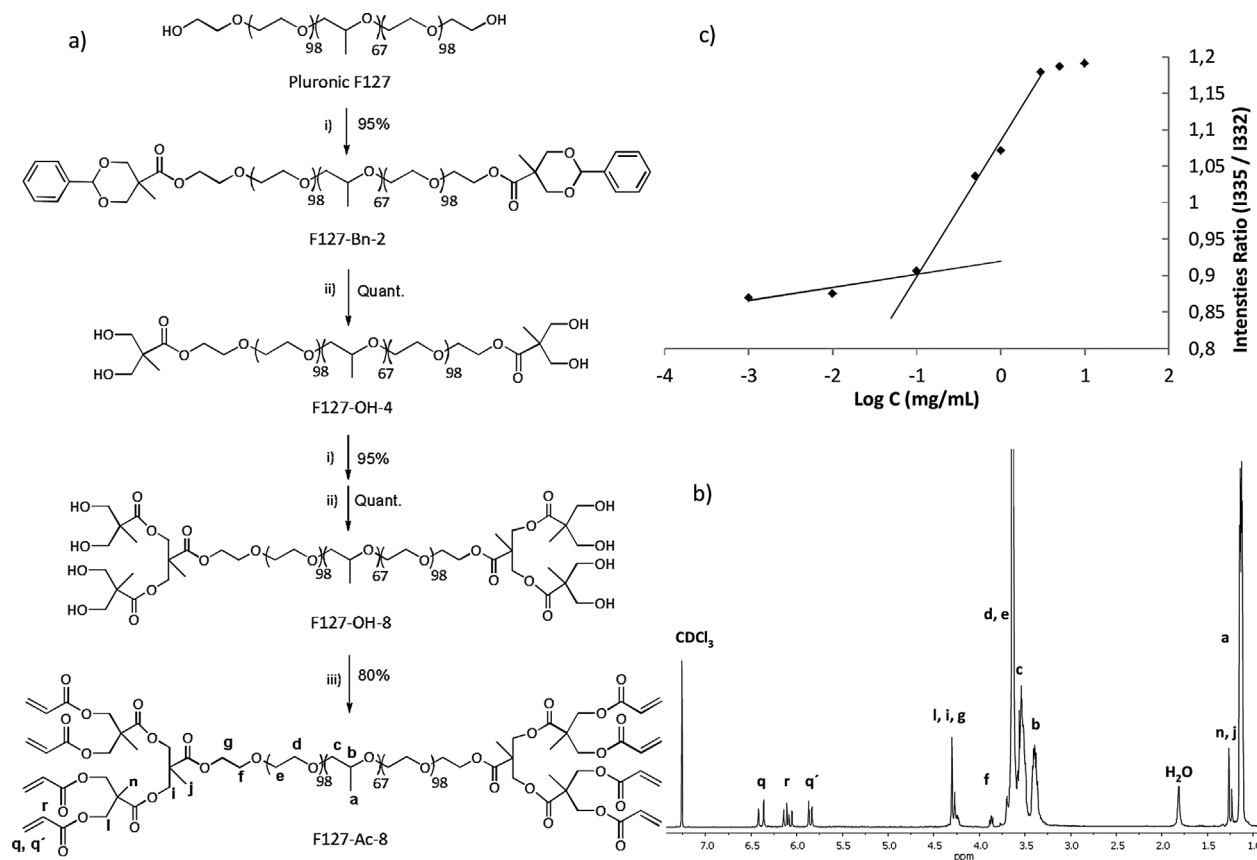


Figure 2. (a) Synthesis of F127-Ac-8. Reagents and reaction conditions: (i) benzylidene-2,2-bis(oxyethyl) propionic anhydride, DMAP, dichloromethane; (ii) Pd/C/H₂, ethyl acetate; (iii) acryloyl chloride, TEA, dichloromethane. (b) ¹H-NMR spectra of F127-Ac-8 in CDCl₃, 300 MHz. (c) CMC calculation: intensities ratio I_{335}/I_{332} versus log concentration (log C) of F127-Ac-8.

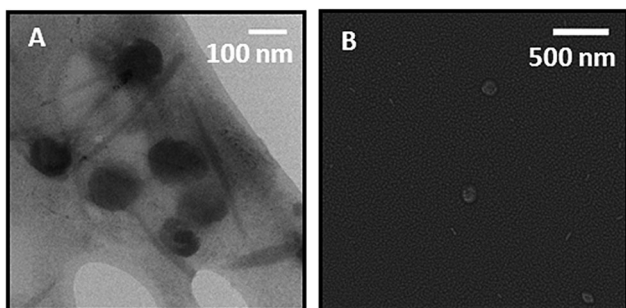
ends of commercial Pluronic F127 (Figure 2a). The synthetic pathway consists of five steps that provide each intermediate with high yields after easy purification processes when needed, i.e., F127-Bn-2, F127-Bn-4, and F127-Ac-8 were precipitated with cold diethyl ether from the reaction mixture, and F127-OH-4 and F127-OH-8 were used as obtained without further purification.

The terminal hydroxyl groups of Pluronic were esterified using the benzyl-protected anhydride derived from 2,2-bis(hydroxymethyl) propionic acid. This acylating agent was used in each step to grow the generation of the dendron following a debenzoylation reaction to deprotect the terminal hydroxyl groups of the bis-MPA dendron, as described by Fréchet and co-workers.^[16] In the final stage, the terminal hydroxyl groups of both dendritic blocks were functionalized with acryloyl chloride in the presence of triethylamine. The final compound was fully characterized by ¹H-NMR, ¹³C-NMR, IR, and MALDI-TOF. The complete conversion of the octahydroxy intermediate, F127-OH-8, into the octa-acrylate derivative, F127-Ac-8, was assessed by ¹H-NMR, Figure 2b (see also ESI), with the appearance

and correct integration of the signals corresponding to the protons of the acrylate group, labeled as q, q', and r in Figure 2b.

Finally, the ability of the amphiphilic macromer F127-Ac-8 to self-aggregate in water so as to form micelles was determined by the pyrene method. This method is based on the displacement of the excitation maximum of pyrene from $\lambda_{\max} = 332$ to 335 nm when it is in a hydrophilic or a hydrophobic environment, respectively. Once formed the aggregates, pyrene locates in the hydrophobic core of the micelles and hence the intensity of the excitation maximum at 335 nm (I_{335}) increases in detriment of the band at 332 nm (I_{332}). The representation of the I_{335}/I_{332} intensity ratio versus logarithm of the concentration of pyrene leads to a curve, where CMC is determined by calculating the intersection of the two straight lines.

In order to obtain the corresponding curve, F127-Ac-8 solutions were prepared at 0.001, 0.01, 0.1, 0.5, 1, 3, 5, and 10 mg · mL⁻¹. Then, a similar amount of pyrene was added in each sample, with a final pyrene concentration of 6×10^{-8} M. The excitation spectrum of the samples was



■ Figure 3. (a) TEM image and (b) SEM image for F127-Ac-8 CLPMs.

measured in the range of 300–350 nm with $\lambda_{\text{emission}} = 390$ nm. A critical micellar concentration of $0.11 \text{ mg} \cdot \text{mL}^{-1}$ was determined for F127-Ac-8 (Figure 2c).

2.2. Preparation and Morphological Characterization of CLPMs

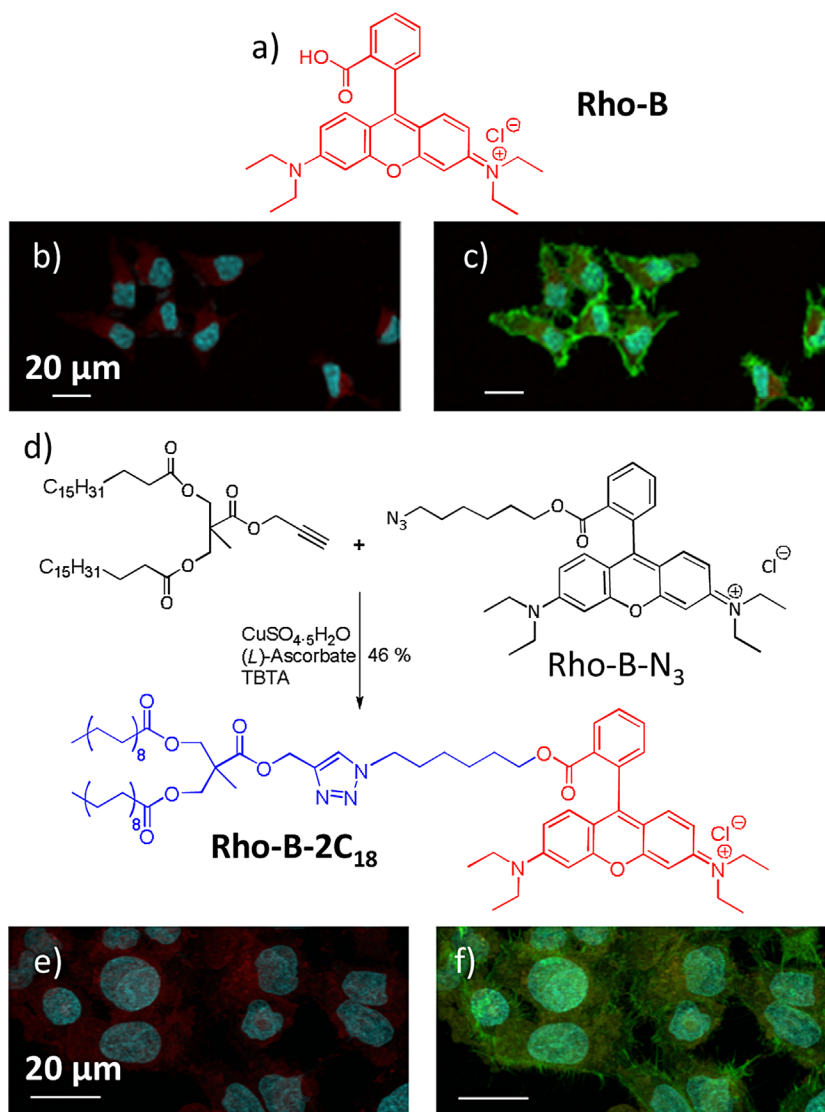
Upon formation of the micelles of F127-Ac-8, these could be stabilized by intramolecular photocross-linking providing stable polymeric nanoparticles.^[3] The photo-induced polymerization was carried out using $7.7 \text{ mg} \cdot \text{mL}^{-1}$ aqueous solutions of the macromer containing $1 \text{ mg} \cdot \text{mL}^{-1}$ of Irgacure 2959 as a biocompatible photoinitiator. The solution was irradiated with UV light, $\lambda = 365$ nm, at 25°C for 10 min.^[3b,17] Subsequent dialysis at 4°C for 72 h, and filtration through $0.2 \mu\text{m}$ cellulose acetate filters yielded a solution of nanoparticles at a final concentration of $1.9 \pm 0.1 \text{ mg} \cdot \text{mL}^{-1}$, which was used for further studies.

The so-prepared CLPMs were observed by TEM and SEM, and showed a spherical morphology (Figure 3).

The size of the photo-polymerized particles was studied by DLS. A mean diameter of 127 ± 9 nm (polydispersity: 0.56 ± 0.07) was determined at 25°C , whereas a smaller mean diameter of 102 ± 1 nm (polydispersity: 0.36 ± 0.02) was determined at 37°C . The observed size variation with temperature confirmed that the nanoparticles display thermosensitive behavior, provided by Pluronic-F127. This temperature-dependent feature should also help to validate these CLPMs as suitable candidates for responsive drug carriers.^[18]

2.3. Encapsulation of Fluorescent Probes and Cell-Uptake Studies

For cell-uptake studies of the F127-Ac-8 CLPMs, water-soluble rhodamine B [Rho-B] (Figure 4a) was first used as a fluorescent probe. The encapsulation of Rho-B into the CLPM was carried out by the solvent evaporation method, using ethanol as the volatile solvent. Rho-B was dissolved in ethanol at $0.15 \text{ mg} \cdot \text{mL}^{-1}$ concentration. A $0.15 \text{ mg} \cdot \text{mL}^{-1}$ solution of Rho-B was added over CLPMs F127-Ac-8 solution at a feed ratio of 0.15 mg of Rho-B $\cdot \text{mg}^{-1}$ of CLPM. The



■ Figure 4. (a) Chemical structure of rhodamine B; (b) and (c) confocal microscopy images for HeLa cells incubated with Rho-B-loaded nanoparticles. (d) Chemical structure of the derivative of rhodamine B incorporating a hydrophobic block, Rho-B-2C₁₈; (e) and (f) confocal microscopy images for HeLa cells incubated with Rho-B-2C₁₈-loaded nanoparticles. (b) and (e) images correspond to cellular nuclei stained with DAPI in blue and Rho-B or Rho-B-2C₁₈ appear in pink. (c) and (f) images exhibit also the green fluorescence due to cytoskeleton stained with Alexa Fluor 488 Phalloidin.

mixture was incubated at room temperature for 24 h. Ethanol was evaporated with orbital agitation. After dialysis for 24 h, the amount of encapsulated Rho-B was calculated indirectly as the difference between the initial quantity of Rho-B added and the amount of Rho-B present in the dialysis solution, determined by fluorescence. Accordingly, an encapsulation efficiency (EE) of 50.6% was calculated.^[28]

Cell-uptake experiments were performed on HeLa cells. The cells were incubated with a solution of $0.6 \text{ mg} \cdot \text{mL}^{-1}$ Rho-B loaded CLPMs for 4 h at 37°C . For the co-localization of Rho-B labeled CLPMs using confocal microscopy, staining of actin was performed with Alexa Fluor 488 Phalloidin. Confocal images (Figure 4b and c) suggest that F127-Ac-8 CLPMs allow the accumulation of Rho-B within the cell. Nevertheless, since Rho-B is highly soluble in water, it is still possible that, in the high dilution conditions of culture media, Rho-B releases from the nanoparticles and enters into the cells by simple diffusion induced by a concentration gradient.

In order to prevent fast release of the fluorescent probe from the CLPMs during the experiment time, a newly designed Rho-B fluorescent probe [Rho-B-2C₁₈], which contains a hydrophobic block that confers it negligible solubility in water, was designed (Figure 4d). Rho-B-2C₁₈ was synthesized by copper-catalyzed 1,3-dipolar azide-alkyne cycloaddition between an azide derivative of rhodamine-B and a first generation *bis*-MPA dendron functionalized by esterification of the hydroxyl groups with stearic acid.

The encapsulation of Rho-B-2C₁₈ was carried out using the same methodology described for Rho-B. The analysis of the dialysis solution revealed the absence of Rho-B-2C₁₈, yielding an EE of 100%, likely due to the enhanced interactions between its hydrophobic block and the hydrophobic regions in the CLPM. Cell-uptake experiments were performed under the same conditions as for Rho-B loaded CLPMs. Similarly, confocal images showed accumulation of fluorescence within the cell after 4 h incubation at 37°C (Figure 4e and f), thus confirming internalization of nanoparticles into the cells.

2.4. Camptothecin Encapsulation

In order to explore the possibility of these CLPMs to act as nanocarriers for anti-HCV drugs, we undertook cytotoxicity and anti-HCV activity experiments based on encapsulated CPT.

Due to the insolubility of CPT in volatile water-soluble solvents, the evaporation method could not be employed for the encapsulation. Instead, a solution ($0.15 \text{ mg} \cdot \text{mL}^{-1}$) of CPT in DMSO was added into the F127-Ac-8 CLPMs solution ($1.9 \pm 0.1 \text{ mg} \cdot \text{mL}^{-1}$) until a ratio of 0.15 mg of CPT per mg of CLPM was reached. The mixture was incubated at room temperature for 24 h. DMSO was eliminated by dialysis

(Spectra/Por MWCO 2000, Spectrum), causing non-encapsulated CPT precipitation. The elimination of non-encapsulated CPT was carried out by filtration with $0.45 \mu\text{m}$ Teflon filters. Encapsulated CPT quantification was made directly by taking $5 \mu\text{L}$ of filtered solution, which was previously lyophilized and re-dissolved in a known volume of DMSO. CPT was quantified by fluorescence emission spectrum ($\lambda_{\text{max}} = 436 \text{ nm}$ in DMSO with $\lambda_{\text{exc}} = 368 \text{ nm}$) by using a calibration curve in the concentration range $11.2\text{--}39.2 \mu\text{g} \cdot \text{mL}^{-1}$ in DMSO. The final concentrations of the solution were $0.42 \text{ mg} \cdot \text{mL}^{-1}$ of CLPMs and $18.8 \mu\text{g} \cdot \text{mL}^{-1}$ of CPT. This result corresponds to an EE% of 32.7%,^[28] a drug loading content of 4.5% and a loading capacity of $44.6 \mu\text{g}$ of CPT $\cdot \text{mg}^{-1}$ of F127-Ac-8 CLPMs.

The encapsulation process of CPT within the F127-Ac-8 CLPMs was studied by isothermal titration calorimetry, ITC. Experiments were performed at 25°C in aqueous media with 3% of DMSO to increase solubility. $100 \mu\text{M}$ CPT solution in the calorimetric cell was titrated with F127-Ac-8 polymer $30 \mu\text{M}$ solution. Control experiments were performed under the same experimental conditions. The heat evolved after each ligand injection was obtained from the integral of the calorimetric signal (Figure 5).

The association constant (K_a) and the enthalpy change (ΔH) were obtained through non-linear regression of experimental data to a model considering one class of ligand-binding sites. The results reflected that CPT encapsulation is energetically favored with an association constant $K_a = 1.5 \cdot 10^7 \text{ M}^{-1}$, corresponding to a moderate-to-high Gibbs energy of interaction ($\Delta G = -9.8 \text{ kcal} \cdot \text{mol}^{-1}$) dominated by the entropic contribution ($-T\Delta S = -16.6 \text{ kcal} \cdot \text{mol}^{-1}$), with an unfavorable interaction enthalpy ($\Delta H = 6.8 \text{ kcal} \cdot \text{mol}^{-1}$), as expected for a predominantly hydrophobic interaction between the drug and the hydrophobic region of the CLPMs. Thus, the F127-Ac-8 CLPM-drug calorimetric titrations show that CPT interacts specifically with F127-Ac-8.

2.5. In-vitro Anti-HCV Studies

Once confirmed cell internalization of the CLPMs to deliver a cargo and the possibility of loading CPT into these nanoparticles, the next step was to study the efficacy of the CPT-carrier system as for the inhibition of HCV replicon.

Nevertheless, prior to this study and in order to check the cytotoxicity of the system, we performed cell viability studies on HeLa cells for a range of concentrations of free CPT and F127-Ac-8/CPT CLPMs, close to those used in subsequent antiviral experiments. Figure 6 represents the viability of HeLa cells upon incubation for 3 d. The results show that the cytotoxic effect of free CPT is reduced when CPT is encapsulated into F127-Ac-8 CLPMs. The CC50 of encapsulated CPT is $0.32 \pm 0.03 \mu\text{M}$, compared to 0.26 ± 0.03 for free CPT.

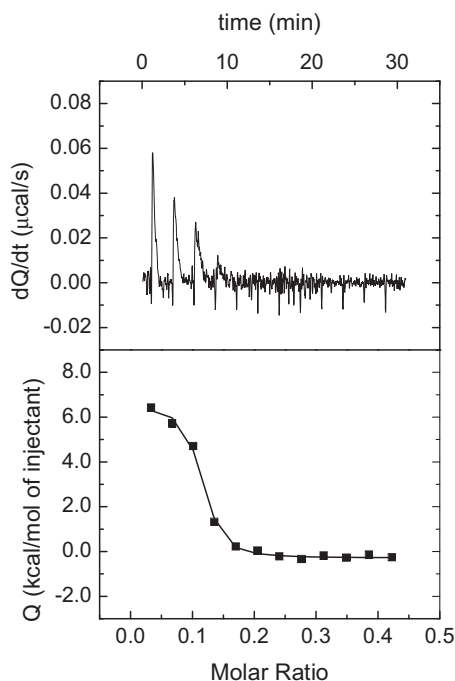


Figure 5. Camptothecin/F127-Ac-8 interaction by isothermal titration calorimetry. Calorimetric titrations were performed by programming sequential injections of camptothecin solution ($0.035 \text{ mg} \cdot \text{mL}^{-1}$) into F127-Ac-8 solution ($0.42 \text{ mg} \cdot \text{mL}^{-1}$) in the calorimetric cell. Upper plot shows the thermogram (thermal power to maintain a zero temperature difference between the reference and sample cells as a function of time) and lower plot shows the binding isotherm (normalized heat per injection as a function of molar ratio). From a simple analysis considering n identical and independent binding sites for CPT in a given F127-Ac-8 nanoparticle, the equilibrium association constant ($K_a = 1.5 \cdot 10^7 \text{ M}^{-1}$) and the interaction enthalpy ($\Delta H = 6.8 \text{ kcal} \cdot \text{mol}^{-1}$) could be estimated.

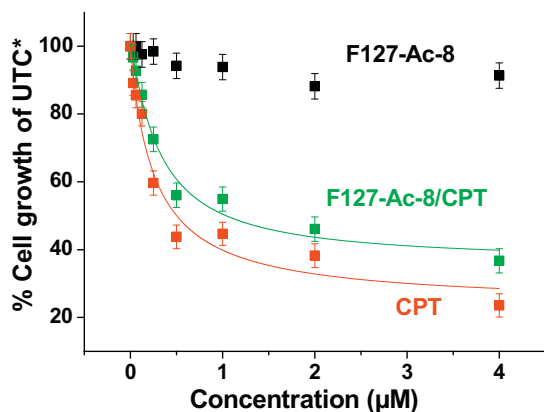


Figure 6. Cell viability for F127-Ac-8 CLPMs on HeLa cells: free F127-Ac-8 CLPMs (black), F127-Ac-8/CPT CLPMs (green), and free CPT (red). Continuous lines are non-linear fittings to the dose-response equation.

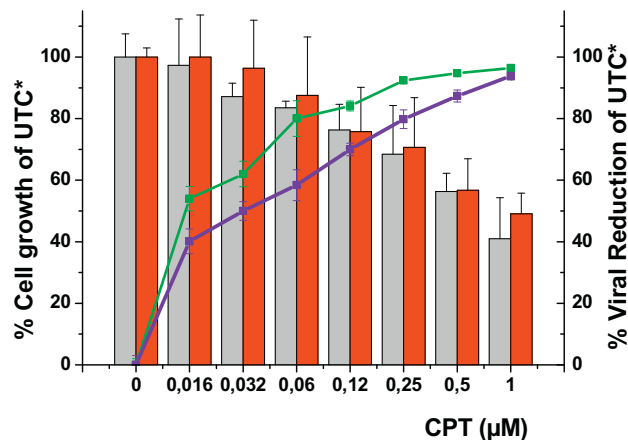


Figure 7. Inhibition of HCV replicon in Huh5-2 cells. Evaluation of potency and cytotoxicity in Huh5-2 cells. Cell survival (bars) and HCV replicon replication rate (lines and symbol) were assessed in cell culture at increasing compound concentration to determine CC₅₀ and EC₅₀: free CPT (grey bars and green line) and F127-Ac-8/CPT CLPMs (red bars and violet line). *UTC: untreated controls.

For inhibition of HCV replicon assays, Huh 5-2 cells were incubated with a control of free CPT and F127-Ac-8/CPT CLPMs. Cell viability data for Huh 5-2 and % of viral load reduction are represented in the same double axis graph (Figure 7).

For both cell types (HeLa and Huh 5-2), a slight decrease in toxicity of F127-Ac-8/CPT CLPMs in comparison to free CPT was observed (Figure 6 and 7). Also, the anti-HCV activity was not the result of a cytostatic or cytotoxic effect, since cell viability remained near 100% at the EC₅₀ values. Non-loaded F127-Ac-8 CLPMs, at the same conditions, did not promote any effect in the virus replication cycle or viability (data not shown). The behavior of free CPT and F127-Ac-8/CPT CLPMs is very similar, and their EC₅₀ values, i.e., 0.013 ± 0.002 and $0.032 \pm 0.01 \mu\text{M}$, respectively, are very close in nanomolar order. Interestingly, cell viability is always slightly higher for encapsulated CPT; in particular, an increase from 40 ± 10 to $50 \pm 7\%$ of the initial cell viability can be observed at $1 \mu\text{M}$ concentration, when the viral load has been nearly totally reduced. This would be specially interesting if CPT is intended as an antiviral agent, instead of an antitumor drug (its approved pharmaceutical application based on its high cytotoxicity in mammalian cells).^[19]

3. Conclusion

In conclusion, these results open new possibilities for the molecular design of cross-linked polymeric micelles for antiviral therapy applications. Particularly, the macromer F127-Ac-8, with a hybrid dendritic-linear-dendritic block copolymer structure provides a molecular design that takes

advantage of the amphiphilic nature of Pluronic and the multivalency provided by the dendritic blocks to achieve micelle stabilization by photocross-linking and high loading capacity. The cytotoxicity of the drug is reduced when encapsulated, while the same efficacy of the free drug against the hepatitis-C virus is maintained. Interestingly, the multivalency of this dendritic block molecule can be exploited toward the multiconjugation of the polymeric micelles with active groups such as targeting moieties, offering future prospects for this sort of amphiphilic reactive compounds.

4. Experimental Section

4.1. Materials

Pluronic F127 (average $M_w = 12\,600$), acryloyl chloride, 4-dimethyl-aminopyridine (DMAP), 2,2-bis(hydroxymethyl) propionic acid (*bis*-MPA), acryloyl chloride, triethylamine (TEA), 1,3-dicyclohexylcarbodiimide (DCC), benzaldehyde dimethyl acetal, *p*-toluenesulfonic acid monohydrate, 2-hydroxy-1-(4-(hydroxyethoxy) phenyl)-2-methyl-1-propanone (Irgacure 2959, I2959), rhodamine B, $\text{CuSO}_4 \cdot 5\text{H}_2\text{O}$, (l)-ascorbate, and camptothecin were obtained from Sigma–Aldrich. Pluronic F127 was dried during 3 h at 100°C under vacuum prior to use. All solvents were purchased from Sigma–Aldrich. 4-(dimethylamino) pyridinium 4-toluenesulfonate (DPTS), 6-azido-hexan-1-ol, 2-(but-3-ynoyl)-2-methylpropane-1,3-diyl distearate ($\text{HC}\equiv\text{C}-2\text{C}_{18}$)^[11] and tris(benzyltriazolylmethyl) amine^[20] (TBTA) were synthesized according to previously reported procedures.

DMEM (Dulbeccó's modified Eagle's medium, $4.5\text{ g}\cdot\text{L}^{-1}$ glucose), DPBS (Dulbecco's phosphate-buffered saline), l-glutamine, $1\times$ non-essential amino acids, Geneticin (G418), and Alamar Blue reagent were purchased from Gibco. Penicillin/streptomycin ($5\,000\text{ U}\cdot\text{mL}^{-1}$), amphotericin B ($250\text{ }\mu\text{g}\cdot\text{mL}^{-1}$), and trypsin (trypsin–versene $10\times$) were obtained from Lonza. Alexa-Fluor488-labeled-phalloidin and DAPI (4',6-diamidino-2-phenylindole, dilactate) were purchased from Invitrogen. Paraformaldehyde (PFA) and bovine serum albumin (BSA) were supplied by Sigma–Aldrich. Mowiol and saponin from Merck Millipore. Fetal bovine serum (PAN-Biotech GmbH, Germany). Bright-Glo™ Luciferase Assay System (Promega Corporation), CellTiter 96 Aqueous One Solution Cell Proliferation Assay (Promega Corporation).

4.2. Synthesis and Characterization of F127-Ac-8

4.2.1. F127-Bn-2

Pluronic F127 (10.0 g, 0.79 mmol) was dissolved in dry dichloromethane (20 mL). DMAP (0.12 g, 0.95 mmol) and benzylidene-2,2-bis(oxyethyl) propionic anhydride (2.0 g, 4.76 mmol) were added. The mixture was stirred at room temperature overnight. The excess of anhydride was quenched by adding methanol (6 mL). The mixture was stirred overnight and the crude was precipitated in cold diethyl ether (1 L). The product was isolated as a white powder after filtration. Yield: 95%. $^1\text{H-NMR}$ (400 MHz, CDCl_3 , δ): 1.04 (s, 6H,

$-\text{CH}_3$), 1.13 (m, 201H, $-\text{CH}_3$), 3.37–3.82 (m, $\approx 1\,100\text{H}$, $-\text{O}-\text{CH}_2-\text{CH}_2-\text{O}-$), 4.35 (m, 4H, $-\text{CH}_2-\text{CH}_2-\text{OC}(\text{O})-$), 4.66 (d, $J = 11.6\text{ Hz}$, 4H, $-\text{CH}_2-\text{OC}(\text{O})-$), 5.44 (s, 2H, $-\text{CH}-\text{Ph}$), 7.32 (m, 6H, Ar H), 7.42 (m, 4H, Ar H); $^{13}\text{C-NMR}$ (100 MHz, CDCl_3 , δ): 17.3, 17.4, 17.9, 42.4, 64.2, 68.5, 68.6, 69.1, 70.5, 72.9, 73.3, 75.1, 75.3, 75.5, 101.7, 126.2, 128.2, 128.9, 137.9, 173.9; IR (molten polymer over NaCl): $\nu = 2\,883$ (C–H st), 1 737 (C=O st), 1 114 (C–O–C st) $\cdot\text{cm}^{-1}$; MALDI⁺ maximum m/z 5050.2 and 13297.2. Anal. calcd. for $\text{C}_{621}\text{H}_{1220}\text{O}_{272}$: C 57.29, H 9.38; found: C 56.68, H 9.55.

4.2.2. F127-OH-4

F127-Bn-2 (9.5 g, 0.73 mmol) was dissolved in ethyl acetate (200 mL). Then, Pd/C (10% by weight) was added. After three vacuum–argon cycles, the reaction mixture was stirred at room temperature in hydrogen atmosphere overnight. The Pd/C was filtered off with Celite and the filtrate was evaporated to give a white solid. Yield: Quant. $^1\text{H NMR}$ (300 MHz, CDCl_3 , δ): 1.11 (s, 6H, $-\text{CH}_3$), 1.13 (m, 201H, $-\text{CH}_3$), 3.37–3.82 (m, $\approx 1\,100\text{H}$, $-\text{O}-\text{CH}_2-\text{CH}_2-\text{O}-$), 4.34 (m, 4H, G, $-\text{CH}_2-\text{CH}_2-\text{OC}(\text{O})-$); $^{13}\text{C NMR}$ (75 MHz, CDCl_3 , δ): 17.1, 17.3–17.4, 49.5, 63.2, 67.3, 68.7, 70.5, 72.9, 73.3, 75.1, 75.3, 75.5, 175.6; IR (molten polymer over NaCl): $\nu = 3\,482$ (OH), 2 884 (C–H st), 1 728 (C=O), 1 112 (C–O–C) $\cdot\text{cm}^{-1}$; MALDI⁺: maximum m/z 5 213.9 and 13 780.1; Anal. calcd. for $\text{C}_{607}\text{H}_{1212}\text{O}_{272}$: C 56.42, H 9.44; found: C 56.04, H 9.98.

4.2.3. F127-Bn-4

F127-OH-4 (4 g, 0.31 mmol) was dissolved in dry dichloromethane (15 mL). Benzylidene-2,2-bis(oxyethyl) propionic anhydride (2.13 g, 4.99 mmol) and DMAP (122 mg, 1 mmol) were added after dissolution. The reaction was stirred at room temperature for 72 h. The excess of anhydride was quenched by adding methanol (6 mL). The mixture was stirred for 7 h and the crude was precipitated in cold diethyl ether (1 L). The product was isolated after filtration as white solid. Yield: 95%. $^1\text{H NMR}$ (300 MHz, CDCl_3 , δ): 0.93 (s, 12H, $-\text{CH}_3$), 1.13 (m, 201H, $-\text{CH}_3$), 1.24 (s, 6H, $-\text{CH}_3$), 3.37–3.82 (m, $\approx 1\,100\text{H}$, $-\text{O}-\text{CH}_2-\text{CH}_2-\text{O}-$, and $-\text{CH}_2-\text{OC}(\text{O})-$), 4.11 (m, 4H, $-\text{CH}_2-\text{CH}_2-\text{OC}(\text{O})-$), 4.37 (s, 8H, $-\text{CH}_2-\text{OC}(\text{O})-$), 4.56 (d, $J = 11.5\text{ Hz}$, 8H, $-\text{CH}_2-\text{OC}(\text{O})-$), 5.40 (s, 4H, $-\text{CH}-\text{Ph}$), 7.28 (m, 12H, Ar H), 7.38 (m, 8H, Ar H); $^{13}\text{C-NMR}$ (75 MHz, CDCl_3 , δ): 17.4, 17.6, 17.7, 42.5, 46.7, 64.1, 65.4, 68.5, 70.5, 72.9–73.3, 75.1–75.3–75.5, 101.6, 126.1, 128.0, 128.8, 137.7, 173.1; IR (molten polymer over NaCl): $\nu = 2\,883$ (C–H st), 1 741 (C=O), 1 113 cm^{-1} (C–O–C). MALDI⁺: maximum m/z 5 615.9 and 13 844.4. Anal. calcd for $\text{C}_{655}\text{H}_{1260}\text{O}_{284}$: C 57.59, H 9.23; found: C 56.89, H, 9.74.

4.2.4. F127-OH-8

F127-Bn-4 (2.8 g, 0.21 mmol) was dissolved in ethyl acetate (100 mL). Then, Pd/C (10% by weight) was added. After three vacuum–argon cycles, the reaction mixture was stirred at room temperature in hydrogen atmosphere overnight. The Pd/C was filtered off with Celite and the filtrate was evaporated to give the product as a white solid. Yield: Quant. $^1\text{H-NMR}$ (400 MHz, CDCl_3 , δ): 1.05 (s, 12H, $-\text{CH}_3$), 1.13 (m, 201H, $-\text{CH}_3$), 1.28 (s, 6H, $-\text{CH}_3$), 3.37–3.79 (m, $\approx 1\,100\text{H}$, $-\text{O}-\text{CH}_2-\text{CH}_2-\text{O}-$), 4.26–4.38 (q, 8H, $\Delta\nu = 35\text{ Hz}$, $J = 11.2\text{ Hz}$, $-\text{CH}_2-\text{OC}(\text{O})-$), 4.26 (m, 4H, $-\text{CH}_2-\text{CH}_2-\text{OC}(\text{O})-$); $^{13}\text{C-RMN}$ (100 MHz, CDCl_3 ,

δ): 17.1, 17.3–17.4, 17.9, 46.4, 49.7, 64.3, 64.9, 67.3–67.4, 68.5–68.8, 70.5, 72.9–73.3, 75.1–75.3–75.5, 172.9, 174.9; IR (molten polymer over NaCl): $\nu = 3457$ (OH), 2884 (C–H st), 1733 (C=O), $1113 \cdot \text{cm}^{-1}$ (C–O–C); MALDI⁺: maximum m/z 5286.1 and 13693.8; Anal. calcd for $\text{C}_{627}\text{H}_{1244}\text{O}_{284}$: C 56.59, H 9.36, found: C 56.17, H 9.98.

4.2.5. F127-Ac-8

F127-OH-8 (1.5 g, 0.11 mmol) was dissolved in dry dichloromethane (20 mL). Then, triethylamine (0.55 mL, 3.98 mmol) and *p*-methoxyphenol (200 mg, polymerization inhibitor) were added. The reaction was cooled for 10 min in an ice bath and acryloyl chloride (0.29 mL, 3.61 mmol) was added dropwise under argon atmosphere. The mixture was stirred at room temperature for 14 h in the dark. The solution was passed through a neutral alumina column and the filtrate was dried with Na_2CO_3 during 2 h. The product was purified by precipitation in cold diethyl ether (250 mL). The product was obtained after filtration as a white solid. Yield: 80%. ¹H NMR (300 MHz, CDCl_3 , δ): 1.13 (m, 201H, $-\text{CH}_3$), 1.23 (s, 6H, $-\text{CH}_3$), 1.27 (s, 12H, $-\text{CH}_3$), 3.37–3.87 (m, $\approx 1100\text{H}$, $-\text{O}-\text{CH}_2-\text{CH}_2-\text{O}-$), 4.23–4.30 (m, 28H, $-\text{CH}_2-\text{OC}(\text{O})-$, and $-\text{CH}_2-\text{CH}_2-\text{OC}(\text{O})-$), 5.85 (dd, $J_{\text{cis}} = 10.4$ Hz, $J_{\text{gem}} = 1.3$ Hz, 4H, $\text{H}_2\text{C} = \text{CH}-$), 6.10 (dd, $J_{\text{trans}} = 17.3$ Hz, $J_{\text{cis}} = 10.4$ Hz, 4H, $\text{H}_2\text{C} = \text{CH}-$), 6.39 (dd, $J_{\text{trans}} = 17.3$ Hz, $J_{\text{gem}} = 1.3$ Hz, 4H, $\text{H}_2\text{C} = \text{CH}-$); ¹³C NMR (125 MHz, CDCl_3 , δ): 17.3–17.4, 17.7, 45.8, 46.5, 64.9, 65.3–65.6, 68.5–68.7, 70.5, 72.9–73.3, 75.1–75.3–75.5, 127.7, 131.5, 165.4, 171.9–172.0; IR (molten polymer over NaCl): $\nu = 2867$ (C–H st), 1733 (C=O), $1109 \cdot \text{cm}^{-1}$ (C–O–C). MALDI⁺: maximum m/z 5761.4 y 14176.6; Anal. calcd for $\text{C}_{651}\text{H}_{1260}\text{O}_{292}$: C 56.90, H 9.18; found: C 56.48, H 9.66.

4.3. Synthesis and Characterization of Rho-B-2C₁₈

4.3.1. Rho-B-N₃

Rhodamine B (1.00 g, 2.09 mmol) was dissolved in dry dichloromethane (70 mL). 6-azido-hexan-1-ol (602 mg, 4.18 mmol) and DPTS (492 mg, 1.67 mmol) were added after the dissolution. The reaction was stirred at 45 °C under argon atmosphere. DCC (861 mg, 4.18 mmol) was dissolved in dry dichloromethane (10 mL) and was added dropwise to the reaction mixture. It was stirred at 45 °C under argon atmosphere overnight, protected from the light. A white precipitate appeared, which was filtered off. Dichloromethane (20 mL) was added to the filtrate. It was washed once with 100 mL of HCl 1.0 M and twice with 100 mL of brine. The organic phase was dried over anhydrous MgSO_4 and the solvent was evaporated under reduced pressure. The crude product was purified on silica gel (DCM: MeOH = ramp from 10:0 to 9:1) to give a purple solid. Yield: 74%. ¹H NMR (400 MHz, CDCl_3): δ (ppm): 1.32 (t, $J = 8$ Hz, 12H, $\text{N}-\text{CH}_2-\text{CH}_3$), 1.49 (m, 4H, $-\text{CH}_2-\text{CH}_2-\text{CH}_2-\text{CH}_2-$), 1.65 (tt, $J = 12$ Hz, 2H, $\text{N}_3-\text{CH}_2-\text{CH}_2-$), 1.87 (tt, $J = 12$ Hz, 2H, $-\text{CH}_2-\text{CH}_2-\text{O}-$), 3.23 (t, $J = 4$ Hz, 2H, N_3-CH_2-), 3.63 (q, $J = 8$ Hz, 8H, $-\text{N}-\text{CH}_2-\text{CH}_3$), 4.02 (t, $J = 8$ Hz, 2H, $-\text{CH}_2-\text{O}$), 6.82 (d, $J = 4$ Hz, 2H, Ar H), 6.89 (dd, $J = 8$ Hz, $J < 4$ Hz, 2H, Ar H), 7.07 (d, $J = 8$ Hz, 2H, Ar H), 7.30 (dd, $J = 8$ Hz, $J < 4$ Hz, 1H, Ar H), 7.75 (td, $J = 8$ Hz, $J = 4$ Hz, 1H, Ar H), 7.82 (td, $J = 8$ Hz, $J = 4$ Hz, 1H, Ar H), 8.29 (dd, $J = 8$ Hz, $J < 4$ Hz, 1H, Ar H); ¹³C NMR (75 MHz, CDCl_3): δ (ppm) 12.6, 25.4, 26.3, 28.2, 28.6, 46.2, 51.3, 65.5, 96.5, 113.6, 114.3, 126.3, 128.5, 130.0–130.3–130.4, 131.3, 133.1, 133.5, 155.5, 157.7, and 165.1. Note: the counter-ions are a mixture of $\text{C}_7\text{H}_7\text{SO}_3^-$ and Cl^- ; $\text{C}_7\text{H}_7\text{SO}_3^-$ was

observed in ¹H NMR (2.26 (s, 2.4H), 7.07 (d, $J = 8$ Hz, 1.6H), 7.9 (d, $J = 8$ Hz, 1.6H), and ¹³C NMR (21.3, 127.0, 129.7, 139.4, and 158.9)). IR (ATR mode): $\nu = 2928$ and 2852 (C–H st), 2095 (N_3), 1715 (C=O), 1645–1585 $\cdot \text{cm}^{-1}$ (C–C_{ar}). MS (ESI⁺): m/z : $[\text{M}^+]$ calcd for $\text{C}_{34}\text{H}_{42}\text{N}_5\text{O}_3$ 568, 32; found, 568, 39. Anal. calcd for $\text{C}_{34}\text{H}_{42}\text{N}_5\text{O}_3^+$, Cl^- / $\text{C}_7\text{H}_7\text{SO}_3^-$: C 66.8, H 6.7, N 9.9, S 3.5; found: C 66.3, H 7.0, N 10.0, and S 3.7.

4.3.2. Rho-B-2C₁₈

Rho-B-N₃ (200 mg, 0.33 mmol) and $\text{HC}\equiv\text{C}-2\text{C}_{18}$ (280 mg, 0.40 mmol) were dissolved in dry dimethylformamide (7 mL) and the mixture was stirred at 45 °C. Three cycles of vacuum–argon were made to remove O₂. $\text{CuSO}_4 \cdot 5\text{H}_2\text{O}$ (9.8 mg, 0.03 mmol), (I)-ascorbate (13.1 mg, 0.07 mmol), and TBTA (17.6 mg, 0.003 mmol) were dissolved in dry dimethylformamide (3 mL) and the mixture was stirred at 45 °C. Three cycles of vacuum–argon were made to remove O₂. After 15 min, the Cu(I) solution was added to the first one through a canula. Three cycles of vacuum–argon were made to remove O₂. The reaction mixture was stirred at 45 °C for 24 h protected from the light. A mixture of brine and water (1:1) (100 mL) was added to the reaction mixture. The product was extracted three times with ethyl acetate (3 \times 70 mL). The organic phases were dried over anhydrous MgSO_4 and the solvent was evaporated under reduced pressure. The crude product was purified on silica gel (DCM: MeOH = ramp from 100:0 to 92:8) to give a purple solid. Yield: 46%. ¹H NMR (400 MHz, CDCl_3 , δ): 0.87 (t, $J = 6.4$ Hz, 6H, $-(\text{CH}_2)_{17}-\text{CH}_3$), 1.24 (m, 71H, $-\text{CH}_2-\text{CH}_2-\text{CH}_2-\text{CH}_2-$, $-(\text{CH}_2)_{14}-\text{CH}_3$), 1.33 (t, $J = 8$ Hz, 12H, $-\text{N}-\text{CH}_2-\text{CH}_3$), 1.44 (m, 2H, $-\text{CH}_2-\text{CH}_2-\text{O}-$), 1.56 (m, 4H, $-(\text{CH}_2)_{14}-\text{CH}_2-\text{CH}_2-\text{C}(\text{O})\text{O}-$), 2.25 (t, $J = 7.2$ Hz, 4H, $-(\text{CH}_2)_{14}-\text{CH}_2-\text{CH}_2-\text{C}(\text{O})\text{O}-$), 3.63 (q, $J = 6.8$ Hz, 8H, $-\text{N}-\text{CH}_2-\text{CH}_3$), 4.01 (t, $J = 6$ Hz, 2H, $-\text{CH}_2-\text{CH}_2-\text{O}-$), 4.21 (AB, 4H, $-\text{CH}_2-\text{O}-$), 4.43 (t, $J = 5.6$ Hz, 2H, $-\text{C}_2\text{H}_4\text{N}_3-\text{CH}_2-\text{CH}_2-$), 5.25 (s, 2H, $-\text{O}-\text{CH}_2-\text{C}_2\text{H}_4\text{N}_3-$), 6.95 (m, 4H, Ar H), 7.10 (d, $J = 8$ Hz, 2H, Ar H), 7.30 (d, $J = 8$ Hz, 1H, Ar H), 7.35 (s, 1H, $-\text{C}_2\text{H}_4\text{N}_3-$), 7.77 (m, 2H, J, Ar H), 8.30 (d, $J = 8$ Hz, 1H, Ar H), note: the signal of the protons $-\text{C}_2\text{H}_4\text{N}_3-\text{CH}_2-\text{CH}_2-$ (near 1.90 ppm) is overlapped with water signal and cannot be observed; ¹³C NMR (75 MHz, CDCl_3 , δ): 12.6, 14.1, 17.8, 22.6–24.9, 25.2, 26.2, 28.1, 28.0, 29.0–29.2–29.3–29.4–29.6–30.0–31.9–34.0, 46.3, 50.7, 64.9, 65.5, 95.6, 113.6, 114.3, 119.1, 124.3, 126.3, 128.5, 130.0–130.3–130.4, 131.3, 133.0, 133.4, 155.5, 157.7, 165.1, 172.6, 173.2; IR (ATR mode): $\nu = 2916$ –2851 (C–H st), 1740–1715 (C=O), 1649–1587 $\cdot \text{cm}^{-1}$ (C–C_{ar}), note: a peak corresponding to water is observed at 3406 cm^{-1} . MALDI⁺: m/z (%) 1273.1 (100) $[\text{C}_{78}\text{H}_{122}\text{N}_5\text{O}_8, \text{H}_2\text{O}]^+$.

4.4. Chemical Characterization Techniques

The ¹H NMR and ¹³C NMR spectra were recorded from their corresponding solutions in CDCl_3 , operating at 300/75 MHz (Bruker AMX300) or 400/100 MHz (Bruker AV-400). IR spectra (Thermo Nicolet Avatar 360 FT-IR spectrometer) of F127-Bn-2, F127-OH-4, F127-Bn-4, F127-OH-8, and F127-Ac-8 were registered from molten polymer over a NaCl tablet, whereas IR spectra (JACS FT/IR-4100) of Rh-B-N₃ and Rh-B-2C₁₈ were registered in ATR mode. Mass spectrometry was performed using an ESI Bruker Esquire 3000 plus spectrometer for Rh-B-N₃ and with a MALDI/TOF-MS Bruker Microflex system for the rest of the products. Elemental analysis was obtained in a microanalyzer Perkin Elmer CHN 2400. GPC was performed in a Waters 2695 apparatus equipped to a light scattering detector Waters 2424.

4.5. Preparation of CLPMs

A 10% (w/v) solution of F127-Ac-8 containing 0.1% of photoinitiator I2959 was prepared in distilled water and kept overnight at 4 °C for complete dissolution of the polymer. The final solution was filtered through a 0.2 µm acetate cellulose filter to remove possible particles in suspension. By dilution with filtered distilled water containing 0.1% of photoinitiator, 0.77% (w/v) solutions were prepared, which were used for photopolymerization. 0.77% precursor solutions were equilibrated for 1 h at room temperature. 5 mL of 0.77% precursor solutions was light cured in a 6 cm diameter cylindrical glass container, using UV light ($\lambda = 365$ nm, 25 °C, 10 min) with a distance of 8 cm between the lamp and the sample. The photopolymerized solution was dialyzed at 4 °C for 72 h, using a cellulose acetate membrane (Spectra/Por Biotech 300,000 MWCO (Spectrum)), with daily water changes. In order to remove larger aggregates, dialyzed samples were filtered with 0.2 µm cellulose acetate filters. To calculate the final concentration, known volumes of this dialyzed and filtered solution of CLPMs were dried by lyophilization in order to weigh the residue. A mean concentration of 1.9 ± 0.1 mg · mL⁻¹ was determined from three freeze-drying experiments.

4.6. CLPM Characterization

4.6.1. Dynamic Light Scattering (DLS)

The size of the CLPMs was measured by DLS at two temperatures, 25 °C and 37 °C, using a Malvern Instrument Nano ZS that uses a He-Ne laser, 633 nm, and a detection angle of 173°.

4.6.2. Transmission Electronic Microscopy (TEM) and Scanning Electronic Microscopy (SEM)

The morphology of the CLPMs was observed by TEM (TECNAI G20, 200 kV) and SEM (Inspect F50). TEM samples were prepared by adding a drop of CLPMs solution in a TEM grid (HOLLEY carbon film 300 mesh Cu, Agar, Scientific). Water from the sample was removed by capillarity with a filter paper. The sample was dried overnight in the darkness. SEM samples were prepared by adding a drop of CLPMs solution in a 12 mm glass coverslip. Sample was allowed to dry overnight in the darkness and gold sputtered before SEM observation.

4.7. Rho-B and Rho-B-2C₁₈ Encapsulation and Loading Content Determination

Rho-B or Rho-B-2C₁₈ was dissolved in ethanol at 0.15 mg · mL⁻¹ concentration. Rho-B or Rho-B-2C₁₈ solution was added over CLPMs F127-Ac-8 solution at a feed ratio of 0.15 mg of Rho-B or Rho-B-2C₁₈ mg⁻¹ of CLPM. The mixture was incubated at room temperature for 24 h. Ethanol was evaporated with orbital agitation.

Aqueous solution containing Rho-B-loaded CLPMs was dialyzed (Slide-A-Lyzes dialysis Cassette G2 2,000 MWCO, Thermo Scientific) with distilled water for 24 h to remove the non-encapsulated Rho-B. Non-encapsulated Rho-B quantification was carried out by fluorescence ($\lambda_{\text{max}} = 576$ nm in water) by using a calibration curve in the concentration range of 2.5–38 µg · mL⁻¹ in water. The amount of encapsulated Rho-B was calculated indirectly as the

difference between the initial feed of Rho-B added and the amount of Rho-B present in the dialyzed solution.

For Rho-B-2C₁₈, no further purification was necessary after ethanol evaporation, due to no precipitation of Rho-B-2C₁₈, indicating a complete encapsulation for Rho-B-2C₁₈.

4.8. Camptothecin Encapsulation and Loading Content Determination

CPT was dissolved in DMSO at 0.15 mg · mL⁻¹. The CPT solution was added over a F127-Ac-8 CLPMs solution (1.9 mg · mL⁻¹) at a feed ratio of 0.15 mg of CPT · mg⁻¹ of CLPM. The mixture was incubated at room temperature for 24 h. DMSO was eliminated by dialysis (Spectra/Por MWCO 2000, Spectrum), causing non-encapsulated camptothecin precipitation. Elimination of non-encapsulated CPT was carried out by filtration with 0.45 µm Teflon filters. Encapsulated CPT quantification was made directly by taking 5 µL of filtered solution, which was previously lyophilized and redissolved in a known volume of DMSO. CPT was quantified by fluorescence emission spectrum ($\lambda_{\text{max}} = 436$ nm in DMSO with $\lambda_{\text{exc}} = 368$ nm) by using a calibration curve in the concentration range 11.2–39.2 µg · mL⁻¹ in DMSO.

4.9. In vitro Cellular Uptake

HeLa cells were seeded at a density of $40 \cdot 10^3$ cells per well in 24 multiwell culture plates over sterile glass covers. Cells were grown for 24 h, and then the medium was replaced with 500 µL of Rho-B or Rho-B-2C₁₈ loaded CLPMs solution (0.6 mg · mL⁻¹) (prepared as described before), whose concentration was adjusted by adding DMEM containing 4.5 g · L⁻¹ D-Glucose, during 4 h at 37 °C. Then, CLPMs solution was removed and cells were washed three times with PBS. Fixation of cells was performed by the addition of 300 µL of paraformaldehyde 4% solution and incubation for 20 min at room temperature. Cells were washed two times with PBS. For the co-localization of Rho-B labeled CLPMs, staining of actin was performed with Alexa Fluor 488 Phalloidin. Cells were first permeabilized in PBS + 1% BSA + 0.1% saponin and then incubated with 40 µL of Alexa Fluor 488 Phalloidin diluted in permeabilization solution (1:200) for 1 h at room temperature in the dark. After washing with PBS-BS (PBS + 1% BSA + 0.1% saponin), PBS-B (PBS + 1% BSA) and distilled water, coverslips were mounted and the cell nuclei stained at the same time with 5 µL solution of MOWIOL-DAPI (1:1 000). After drying, coverslips were sealed with nail polish around the edges and stored at 4 °C in the darkness until confocal microscopy observation. Cellular uptake and localization were explored by confocal microscopy using a 60× objective (Olympus FV10-i Oil Type, Olympus, Spain). Green fluorescence was observed under 499/520 (Ex/Em), red fluorescence was observed under 558/575 (Ex/Em) and DAPI under 359/461 (Ex/Em). Image treatment was done with FV10i-SW software (Olympus).

4.10. Isothermal Titration Calorimetry (ITC) Assay

Binding of CPT to F127-Ac-8 polymer was determined with a high-sensitivity isothermal titration VP-ITC microcalorimeter (MicroCal, USA). Experiments were performed at 25 °C in aqueous media with

3% of DMSO to increase solubility. 100 μM compound solution in the calorimetric cell was titrated with F127-Ac-8 polymer 30 μM solution. Control experiments were performed under the same experimental conditions. The heat due to the binding reaction was obtained as the difference between the reaction heat and the corresponding heat of dilution, the latter estimated as a constant heat throughout the experiment, and included as an adjustable parameter in the analysis. Data were analyzed using software developed in our laboratory implemented in Origin 7 (OriginLab, USA).

4.11. Cells and Replicon System

The highly permissive cell clone Huh 7-Lunet, as well as Huh 7 cells containing subgenomic (HCV) replicons I389luc-ubi-neo/NS3-3'/5.1 (Huh 5-2), I377NS3-3'/wt (Huh 9-13), or I389/hygro-ubi-NS3-3'/5.1 (a kind gift from Dr. V. Lohmann and Dr. R. Bartenschlager) has been described recently.^[21–24] Briefly, this system allowed the efficient propagation of genetically modified HCV RNAs (replicons) in a human hepatoma cell line (Huh). The amount of the RNA that has been transcribed and translated is determined through the quantification of a reporter contained in the replicon system (luciferase). The amount of luminescence detected (after adding the substrate specific for this enzyme) is proportional to the virus replication rate.^[21–24] Cells were grown in Dulbecco's modified Eagle's medium (DMEM; Gibco, Belgium) supplemented with 10% heat-inactivated fetal bovine serum (PAN-Biotech GmbH, Germany), $1\times$ non-essential amino acids (Gibco), 100 IU mL^{-1} penicillin (Gibco), $100\ \mu\text{g}\cdot\text{mL}^{-1}$ streptomycin (Gibco), and $250\ \mu\text{g}\cdot\text{mL}^{-1}$ geneticin (G418; Gibco).

4.12. Antiviral Assay with Huh 5-2 Cells

Antiviral assays for assessing the efficacy of the F127-Ac-8/CPT CLPMs system were performed as described in literature.^[21–25] Briefly, Huh 5-2 cells were seeded at a density of $5\cdot 10^3$ cells per well in a tissue culture-treated white 96-well view plate (Techno Plastic Products AG, Switzerland) in complete DMEM supplemented with $250\ \mu\text{g}\cdot\text{mL}^{-1}$ G418. After incubation for 24 h at $37\ ^\circ\text{C}$, medium was removed and twofold serial dilutions in complete DMEM (without G418) of the F127-Ac-8/CPT CLPMs were added in a total volume of 100 μL . After 3 d of incubation at $37\ ^\circ\text{C}$, cell culture medium was removed and luciferase activity was determined using the Bright-Glo Luciferase Assay System (Promega Corporation, the Netherlands). The luciferase signal was measured using a Synergy HT Multimode Reader (BioTek Instruments, Inc., USA). The 50% effective concentration (EC50) was defined as the concentration of compound that reduced the luciferase signal by 50%.

4.13. Cytostatic Assay

Cytostatic assays for assessing the cell viability of the F127-Ac-8/CPT CLPMs were performed as described in the literature.^[21–24] Briefly, HeLa and Huh 5-2 cell lines were seeded at a density of $5\cdot 10^3$ cells per well of a 96-well plate in complete DMEM (with the appropriate concentrations of G418, in case of Huh 5-2). Serial

dilutions of the test compounds in complete DMEM (without G418) were added 24 h after seeding. Cells were allowed to proliferate for 3 d at $37\ ^\circ\text{C}$, after which the cell number was determined by CellTiter 96 AQueous One Solution Cell Proliferation Assay (Promega Corporation). The 50% cytostatic concentration (CC50) was determined employing the dose–response equation (i.e., Hill equation). All the experiments with HeLa and Huh5-2 cells were carried out in triplicate and each experiment was repeated three different days.

Acknowledgements: This work was financially supported by the MINECO-FEDER funds (projects MAT2012-38538-CO3-01, CTQ2012-35692, and BFU2013-47064-P), Miguel Servet Program from Instituto de Salud Carlos III (CP07/00289, CPII13/00017), Fondo de Investigaciones Sanitarias (PI10/00186), and the Gobierno de Aragón-FSE (E04, B89 and B01 research groups). A. L. and R. C-G. thank the MEC for their FPU grants, FPU12/05210 and FPU13/3870, and R.GP and R. C-G. thank the DGA for the EPIF grants, B054/12 and B136/13. Authors would like to acknowledge the use of “Servicios Científico-Técnicos” of CEQMA (UZ–CSIC) and of CIBA (IACS), and the LMA from INA (UZ).

Received: March 17, 2015; Revised: May 14, 2015; Published online: June 5, 2015; DOI: 10.1002/mabi.201500094

Keywords: anti-HCV; camptothecin; cross-linked micelles; dendrimers; pluronic

- [1] a) V. P. Torchilin, *Nat. Rev. Drug. Discov.* **2014**, *13*, 813; b) C. Alvarez-Lorenzo, A. Concheiro, *Chem. Commun.* **2014**, *50*, 7743.
- [2] a) R. Haag, F. Kratz, *Angew. Chem. Int. Ed.* **2006**, *45*, 1198; b) N. Nishiyama, K. Kataoka, *Pharmacol. Ther.* **2006**, *112*, 630; c) K. Letchford, H. Burt, *Eur. J. Pharm. Biopharm.* **2007**, *65*, 259; d) U. Kedar, P. Phutane, S. Shidhaye, V. Kadam, *Nanomed.: Nanotech., Bio. Med.* **2010**, *6*, 714; e) M. Yokoyama, *J. Exp. Clin. Med.* **2011**, *3*, 151; f) N. Li, J. Wang, X. Yang, L. Li, *Colloids Surf. B: Biointerfaces* **2011**, *83*, 237; g) K. Yoncheva, P. Calleja, M. Agüeros, P. Petrov, I. Miladinova, C. Tsvetanov, J. M. Irache, *Int. J. Pharm.* **2012**, *436*, 258.
- [3] a) D. Missirlis, N. Tirelli, J. A. Hubbell, *Langmuir* **2005**, *21*, 2605; b) D. Missirlis, R. Kawamura, N. Tirelli, J. A. Hubbell, *Eur. J. Pharm. Sci.* **2006**, *29*, 120; c) W. I. Choi, G. Tae, Y. H. Kim, *J. Mater. Chem.* **2008**, *18*, 2769; d) J.-Y. Kim, W. I. Choi, Y. H. Kim, G. Tae, S.-Y. Lee, K. Kim, I. C. Kwon, *J. Control. Release* **2010**, *147*, 109; e) M. Di Biase, P. de Leonardi, V. Castelletto, I. W. Hamley, B. Derby, N. Tirelli, *Soft Matter* **2011**, *7*, 4928. f) R. Yang, F. Meng, S. Ma, F. Huang, H. Liu, Z. Zhong, *Biomacromolecules* **2011**, *12*, 3047. g) H. Li, X. Zhang, X. Zhang, B. Yang, Y. Wei, *Colloids Surf. B: Biointerfaces* **2014**, *121*, 347.
- [4] a) C. Khemtong, C. W. Kessinger, J. Gao, *Chem. Commun.* **2009**, 3497; b) T. Sun, Y. S. Zhang, B. Pang, D. C. Hyun, M. Yang, Y. Xia, *Angew. Chem. Int. Ed.* **2014**, *53*, 12320.
- [5] a) X. Li, Q. Wu, Z. Chen, X. Gong, X. Lin, *Polymer* **2008**, *49*, 4769; b) R. Mehendale, M. Joshi, V. B. Patravale, *Crit. Rev. Ther. Drug Carrier Syst.* **2013**, *30*, 1; c) E. F. Craparo, D. Triolo, G. Pitarresi, G. Giammona, G. Cavallaro, *Biomacromolecules* **2013**, *14*, 1838. d) A. A. Smith, M. B. L. Kryger, B. M. Wohl, P. Ruiz-

- Sanchis, K. Zuwala, M. Tolstrup, A. N. Zelikin, *Polym. Chem.* **2014**, *5*, 6407.
- [6] a) Y. H. Hsiang, R. Hertzberg, S. Hecht, L. F. Liu, *J. Biol. Chem.* **1985**, *260*, 14873; b) M. E. Wall, M. C. Wani, C. E. Cook, K. H. Palmer, A. T. McPhail, G. A. Sim, *J. Am. Chem. Soc.* **1966**, *88*, 3888.
- [7] O. Abian, S. Vega, J. Sancho, A. Velázquez-Campoy, *PLoS ONE* **2013**, *8*, e69773.
- [8] a) O. Abian, S. Vega, J. L. Neira, A. Velázquez-Camp Biophys. *J.* **2010**, *99*, 3811; b) O. Abian, J. L. Neira, A. Velázquez-Campoy, *Proteins: Struct., Funct., Bioinf.* **2009**, *77*, 624.
- [9] N. J. Rahier, B. M. Eisenhauer, R. Gao, S. H. Jones, S. M. Hecht, *Org. Lett.* **2004**, *6*, 321.
- [10] a) R. B. Greenwald, A. Pendri, C. Conover, C. Gilbert, R. Yang, J. Xia, *J. Med. Chem.* **1996**, *39*, 1938; b) J. W. Singer, R. Bhatt, J. Tulinsky, K. R. Buhler, E. Heasley, P. Klein, P. de Vries, *J. Control. Release* **2001**, *74*, 243; c) R. Bhatt, P. de Vries, J. Tulinsky, G. Bellamy, B. Baker, J. W. Singer, P. Klein, *J. Med. Chem.* **2003**, *46*, 190; d) Z. Sezgin, N. Yüksel, T. Baykara, *Eur. J. Pharm. Biopharm.* **2006**, *64*, 261; e) J. Wang, R. Wang, L. B. Li, *J. Colloid Interf. Sci.* **2009**, *336*, 808; f) F. Liu, J.-Y. Park, Y. Zhang, C. Conwell, Y. Liu, S. R. Bathula, L. Huang, *J. Pharm. Sci.* **2010**, *99*, 3542; g) N. Li, J. Wang, X. Yang, L. Li, *Colloids Surf. B-Biointerfaces* **2011**, *83*, 237; h) X.-L. Yang, Y.-L. Luo, F. Xu, Y.-S. Chen, *Pharm. Res.* **2014**, *31*, 291; i) Y.-M. Zhang, Y. Cao, Y. Yang, J.-T. Chen, Y. Liu, *Chem. Comm.* **2014**, *50*, 13066; j) P. Ruiz-Sanchis, B. M. Wohl, A. A. A. Smith, K. Zuwala, J. Melchjorsen, M. Tolstrup, A. N. Zelikin, *Adv. Health. Mater.* **2015**, *4*, 65.
- [11] J. Movellan, P. Urbán, E. Moles, J. M. de la Fuente, T. Sierra, J. L. Serrano, X. Fernández-Busquets, *Biomaterials* **2014**, *35*, 7940.
- [12] F. Wurm, H. Frey, *Prog. Polym. Sci.* **2011**, *36*, 1.
- [13] a) A. V. Kabanov, E. V. Batrakova, V. Y. Alakhov, *J. Control. Release* **2002**, *82*, 189; b) A. V. Kabanov, E. V. Batrakova, V. Y. Alakhov, *Adv. Drug Del. Rev.* **2002**, *54*, 759; c) D. A. Chiappetta, A. Sosnik, *Eur. J. Pharm. Biopharm.* **2007**, *66*, 303; d) Z. Wei, J. Hao, S. Yuan, Y. Li, W. Juan, X. Sha, X. Fang, *Int. J. Pharmaceutics* **2009**, *376*, 176–185; e) E. S. Lee, Y. T. Oh, Y. S. Youn, M. Nam, B. Park, J. Yun, J. H. Kim, H.-T. Song, K. T. Oh, *Colloids Surf. B: Biointerfaces* **2011**, *82*, 190; f) F. Z. Dahmani, H. Yang, J. Zhou, J. Yao, T. Zhang, Q. Zhang, *Eur. J. Pharm. Sci.* **2012**, *47*, 179.
- [14] a) E. V. Batrakova, A. V. Kabanov, *J. Control. Release* **2008**, *130*, 98; b) G. Pembouong, N. Morellet, T. Kral, M. Hof, D. Scherman, M.-F. Bureau, N. Mignet, *J. Control. Release* **2011**, *151*, 57.
- [15] A. Carlmark, E. Malmstrom, M. Malkoch, *Chem. Soc. Rev.* **2013**, *42*, 5858.
- [16] H. Ihre, A. Hult, J. M. J. Fréchet, I. Gitsov, *Macromolecules* **1998**, *31*, 4061.
- [17] Y.-C. Wang, J. Wu, Y. Li, J.-Z. Du, Y.-Y. Yuan, J. Wang, *Chem. Commun.* **2010**, *46*, 3520.
- [18] J. Bergueiro, M. Calderón, *Macromol. Biosci.* **2015**, *15*, 183.
- [19] M. E. Wall, M. C. Wani, C. E. Cook, K. H. Palmer, H. T. McPhail, O. A. Sins, *J. Am. Chem. Soc.* **1966**, *88*, 3888.
- [20] T. R. Chan, R. Hilgraf, K. B. Sharpless, V. V. Fokin, *Catalysis* **2004**, *6*, 2853.
- [21] J. Courcambecq, M. Bouzidi, R. Perbost, B. Jouirou, N. Amrani, R. Cacoub, G. Pépe, J.M. Sabatie, P. Halfon, *Antiviral Ther.* **2004**, *11*, 847.
- [22] S. Susser, J. Vermehren, N. Forestier, M. W. Welker, N. Grigorian, C. Füller, D. Perner, S. Zeuzem, C. Sarrazin, *J. Clin. Virol.* **2011**, *52*, 321.
- [23] K. J. Blight, J. A. McKeating, C. M. Rice, *J. Virol.* **2002**, *76*, 13001.
- [24] V. Lohmann, F. Korner, J. Koch, U. Herian, L. Theilmann, R. Bartenschlager, *Science* **1999**, *285*, 110.
- [25] A. Urbani, R. Bazzo, M. C. Nardi, D. O. Cicero, R. De Francesco, C. Steinkühler, G. Barbato, *J. Biol. Chem.* **1998**, *273*, 18760.